NMR Characterization of Structural and Dynamics Perturbations Due to a Single Point Mutation in *Drosophila* DLC8 Dimer: Functional Implications[†]

P. M. Krishna Mohan and Ramakrishna V. Hosur*

Department of Chemical Sciences, Tata Institute of Fundamental Research Homi Bhabha Road, Mumbai 400 005, India

Received March 27, 2008; Revised Manuscript Received April 18, 2008

ABSTRACT: Dynein light chain protein (DLC8), the smallest subunit of the dynein motor complex, acts as a cargo adaptor. The protein exists as a dimer under physiological conditions, and cargo binding occurs at the dimer interface. Dimer stability and relay of perturbations through the dimer interface can thus be anticipated to play crucial roles in the variety of functions the protein performs. Recent investigations point out that DLC8 also gets phosphorylated at Ser 88, which is located at the extreme C-terminal end. In this background, we investigate here by NMR the effects of a small perturbation by way of a single point mutation, S88A, on the structure, dynamics, and cargo binding efficacy of the DLC8 dimer. We observe that the perturbation travels far away along the sequence from the site of the mutation. This relay has been explained at the atomic level by looking into the packing of the side chains in the crystal structure of the protein. It follows that the interface is highly adaptable, which may account for the versatility of the dimer's cargo binding ability. Binding studies with a peptide indicate that the mutation compromises binding efficacy. These observations show how remote residues that may not be directly bound to a target can still affect the affinity of the protein to the target. Furthermore, the S88A mutational perturbations seen here in *Drosophila* DLC8 are dramatically different from those of the same mutation in human DLC8 (also known as DLC1) (Song, C., et al., (2008) *J. Biol. Chem*, *283*, 4004−4013.) which differs from *Drosophila* DLC8 at only five locations. All of these observations put together highlight the sensitivity of dynein light chain protein to small perturbations, and this would have great functional implications.

Cytoplasmic dynein is a microtubule-based multisubunit molecular motor that translocates cargos toward the minus ends of microtubules. Dynein is involved in a wide array of functions including retrograde organelle movement, nuclear migration, miotic spindle alignment and axonal transport (*1–5*). The heavy chain subunits provide ATPase activity essential for force generation and are also responsible for attaching the motor complex to microtubules. The cargo binding domain comprising intermediate and light chain subunits regulate the binding and transport of a wide variety of cargo molecules.

Dynein light chain protein (DLC8[1]) is the smallest (89 amino acids, 10.3 kDa) among the light chains of the dynein motor complex. At physiological pH, the protein exists as a homodimer but dissociates into monomers below pH 4 (*6, 7*). The DLC8 dimer consists of two α-helices (α1, residues 15−31; α2, residues 35−50) and 5 β-strands (β1, residues 6−11; β2, residues 54−59; β3, residues 62−67; β4, residues 72−78; and β5, residues 81−87) (*8*). The dimer binds the target molecules in an antiparallel β-strand fashion through its β3-strand and also forms several contacts with the residues that are present at the dimer interface (*8*). Furthermore, it has been reported that the monomeric DLC8 protein is not capable of binding any of the target molecules (*9*). These facts suggest that the topology of the dimer facilitates cargo loading in the dimer. Other than binding to the intermediate chain (IC74) within the dynein complex, DLC8 interacts also with a large number of cellular targets with diverse biological functions. It interacts with neuronal nitric oxide synthase (nNos) (*10*) proapoptotic BCl-2 family proteins Bim and Bmf (*11, 12*), postsynaptic scaffold proteins GKAP and gephyrin (*13, 14*), nuclear protein p53-binding protein 1 (53BP1) (*15*), and mRNA localization protein Swallow (*16*). The five-residue K/RXTQT sequence has been recognized as one of the common DLC8 recognition motifs in target peptides (*17*). Since DLC8 interacts with various proteins, it was presumed that DLC8 acts as a cargo adaptor in the dynein complex to transport various organelles.

Recent studies on p21-activated kinase 1 (Pak1), a member of the evolutionarily conserved family of serine/threonine kinases, revealed DLC8 as its physiological interacting substrate with binding sites mapped to amino acids 61−89 and the phosphorylation site at Ser 88 (*18*). The phosphorylation of DLC8 by Pak1 plays a regulatory role in tumorigenesis and in macropinocytosis (*18–20*). Pak1 phos-

[†] We thank the Government of India for providing financial support to the National Facility for High Field NMR at the Tata Institute of Fundamental Research. P.M.K.M. is a recipient of TIFR alumni Association Scholarship (2003−2005) and Sarojini Damodaran international fellowship for career development, supported by the TIFR endowment fund.

* To whom correspondence should be addressed. Professor Ramakrishna V. Hosur, Department of Chemical Sciences, Tata Institute of Fundamental Research, Homi Bhabha Road, Mumbai 400 005, India. Tel: 91 22 2278 2488. Fax: 91 22 2280 4610. E-mail: hosur@tifr.res.in.

[1] Abbreviations: DLC8, dynein light chain protein; NMR, nuclear magnetic resonance; HSQC, heteronuclear single quantum coherence; DTT, dithiothreitol; PCR, polymerase chain reaction; SDS−PAGE, sodium dodecyl sulfate−poly acrylamide gel electrophoresis; aa, amino acids; WT, wild type.

10.1021/bi800531g CCC: $40.75
Published on Web 05/09/2008

phorylation of DLC8 on Ser 88 controls vesicle formation and trafficking functions, whereas the mutation of Ser 88 to Ala (S88A) prevents macropinocytosis (*19*). It has also been shown that phosphorylated DLC8 is elevated specifically in human breast cancer tumors (*18*). Furthermore, DLC8 phosphorylation by Pak1 prevents the interaction with apoptotic protein Bim and plays an essential role in cell survival (*18*). It has also been reported that the phosphorylation of DLC8 promotes the dissociation from the intermediate chain (IC74) and hence regulates the assembly of the motor complex (*21*).

All of the above results highlight the importance of the dimer interface in the variety of functions the protein performs. Any perturbation at or near the interface is likely to affect biological function. Thus, often perturbations are introduced deliberately in the form of specific mutations in an attempt to understand the regulatory roles of specific residues involved in target recognition, structural architecture, stability, aggregation, and folding features of the wild type protein (*22–29*). For example, in DLC8, mutations were introduced at His 55 (H55K) to understand the role of charge−charge interaction in the dimer−monomer transition, and at Ser 88 (S88E), the phosphorylation site, to reveal the mechanism of phosphorylation (*21, 30*). The above mutations were found to result in the dissociation of the DLC8 dimer. The same happens when the pH is changed from 7 to 3 (*6*). Even when the dimer remains intact, for some perturbations, it is conceivable that the affinities to different targets and the structural and dynamic features may get altered. These facts must be factored in during interpretation of the effects of any perturbation in understanding biological function.

Intuitively, the remote effects of any perturbation in a protein must be a consequence of a strong network of interactions that may cause a rapid relay of perturbations from any one particular site on the protein structure. However, specific knowledge of how the perturbations travel will be essential in each case to understand the specificities of interactions. Thus, in order to understand these effects at an atomic level in DLC8, we chose to investigate the effects of a single point mutation at the dimer interface that is functionally very important. We monitored the effects of a perturbation almost at the end of the interface, by way of S88A point mutation; alanine is very similar in size to serine but lacks the hydroxyl group in the side chain. Although Ser 88 is present at the extreme C-terminal and at the end of the dimer interface, it is engaged in many H-bond interactions (*8, 21*); the side chain of Ser 88 pairs with the carbonyl of Ser 88′ across the interface (*8*), and the amide group of Gly 89 is very close (∼ 2.6 Å) to the backbone nitrogen of Ser 88, suggesting a possibility of H-bonding. This creates an interesting structural scaffold. Furthermore, the side chain of Ser 88 is packed against many other side chains in the crystal structure of the protein (*8*). All of these indicate that Ser 88 interactions contribute substantially to the stability of the dimeric protein. Furthermore, Ser 88 is highly conserved among various species and is the only recognized phosphorylation site in the dimeric DLC8 (*8, 18*). In this background, the results obtained here provide useful mechanistic insights into the protein's susceptibility to small perturbations on the one hand and a rationale for the remote effects of mutations on the other. As we were preparing this article, a study describing the effects of S88A mutation in the case of DLC1, the human counterpart of DLC8, which differs from DLC8 at only five locations (human, C2, S21, E23, H41, and K71; *Drosophila*, S2, A21, D23, Y41, and R71), was reported (*20*). Interestingly, the two mutant proteins have very different characteristics, although the functional behaviors of the wild type (WT) protein from the two species are similar.

MATERIALS AND METHODS

Mutagenesis and Protein Expression and Purification. The S88A mutant of DLC8 (*Drosophila melanogaster*) was prepared using a standard PCR based protocol of site directed mutagenesis. The mutant DNA was verified by automated sequencing before transformation into BL21 (DE3) cells for protein expression. The wild type (WT) and S88A mutant proteins were expressed and purified as described elsewhere (*6*). The purity of the sample was checked using SDS−PAGE.

Gel Filtration. Gel filtration was performed on the DLC8-WT protein at pH 7 and 3, and on S88A mutant at pH 7 using a Hi Load 16/60 Superdex 75 column (Amersham) with buffer (20 mM Tris, 200 mM NaCl, and 2 mM DTT at pH 7, and 20 mM acetate, 200 mM NaCl, and 2 mM DTT at pH 3) at a flow rate of 0.3 mL/min with absorbance monitored at 280 nm using Bio-Rad BioLogic LP system. Nearly 1 mL of 600 μM protein was loaded on the column.

NMR Spectroscopy. NMR Sample. For NMR studies, the protein purified as described above was concentrated to ∼1.5 mM. Tris buffer (20 mM Tris, 200 mM NaCl, and 2 mM DTT) and acetate buffer (20 mM acetate, 200 mM NaCl, and 2 mM DTT) were used for all the experiments on the dimer (pH 7.0) and on the monomer (pH 3.0), respectively. The final volume in all the samples was ∼550 μl (90% H_2O + 10% D_2O).

NMR Data Acquisition and Processing. All of the NMR experiments were recorded using a triple channel Varian Unity-plus 600 MHz NMR spectrometer equipped with pulse-shaping and pulse-field gradient capabilities. For resonance assignments of S88A mutant, three dimensional (3D) experiments CBCANH and CBCA(CO)NH (*31*) were recorded at pH 7.0 and 27 °C. The ^{1}H and ^{15}N carrier frequencies were set at 4.71 ppm and 119 ppm, respectively, and the ^{13}C carrier frequency was set at 46.0 ppm for CBCANH and CBCA(CO)NH. Amide proton chemical shifts as a function of temperature in the range 20−40 °C were measured by recording seven HSQC spectra (20, 23, 27, 30, 33, 36, and 39 °C) with 256 t_1 increments each. The dimeric proteins (both WT and S88A mutant) and the monomer were stable over the entire temperature range at all chosen pH values. ^{1}H chemical shifts were calibrated relative to 2,2-dimethyl-2-silapentane-5-sulfonate (DSS). The relaxation experiments were carried out using the pulse sequences described by Farrow et al. (*32*). For these experiments, 2048 and 128 complex points were collected along the two dimensions. ^{15}N R_2 measurements were done using the following Carr-Purcell-Meiboom-Gill (CPMG) delays: 10, 30, 50, 70, 90, 110, 130, 150, 190, and 230 ms, and spectra duplicated at 50 and 90 ms. Steady state ^{1}H-^{15}N NOE experiments were carried out using an irradiation time of 3 s and a total recycle delay of 5 s for each scan. Forty-eight scans were used for each fid for signal averaging the data. Peptide binding NMR experiments were carried out at

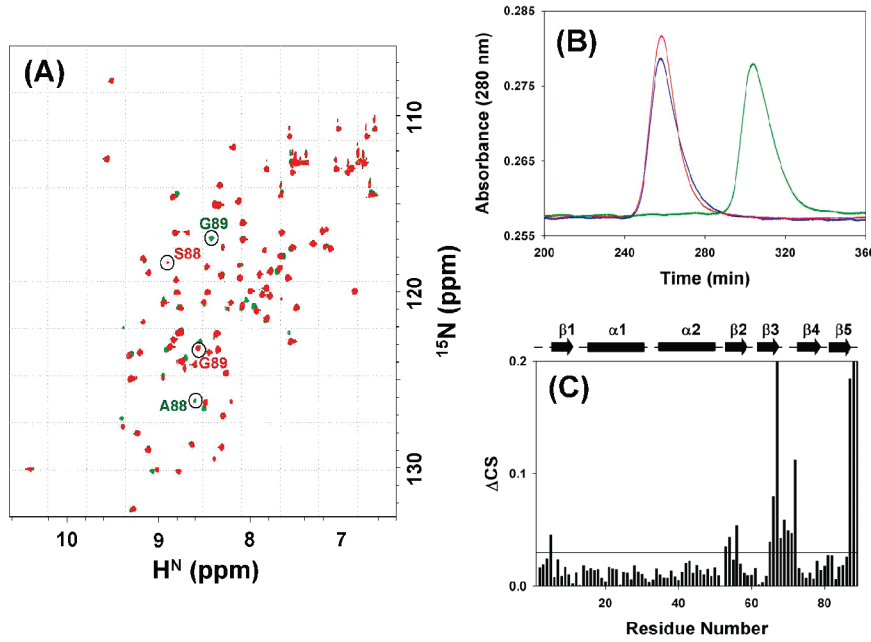

FIGURE 1: (A) Overlay of $^1H^N$-^{15}N HSQC spectra of DLC8 protein at pH 7 and 27 °C [wild type-WT (red) and S88A mutant (green)]: The peaks corresponding to Ser 88 and Gly 89 in WT, and Ala 88 and Gly 89 in S88A mutant are annotated with their respective color codes and are also encircled. (B) Gel filtration data DLC8 WT (blue) and S88A mutant (red) at pH 7. The single and identical peak seen at the same position in the chromatogram indicates that the protein is a pure dimer in both cases. Here, the data of DLC8 protein at pH 3 (green) where the protein is a pure monomer is included as a reference. (C) Residue-wise summed chemical shift changes ($\Delta\delta$) between the WT and S88A mutant of DLC8 protein calculated from ΔH^N and ΔN shifts (see text). The secondary structural elements in the protein are marked above with cylinders (for helices) and arrows (for sheets).

pH 7 and 27 °C, using a commercially synthesized 11 residue peptide fragment (VYTKQTQTTST) of the dynein intermediate chain (IC74) (GL Biochem Ltd.).

All of the data were processed using FELIX on a Silicon Graphic, Inc. work station. Prior to Fourier transformation and zero-filling, data was apodized with a sine-squared weighting function, shifted by 60° in both dimensions for 2D, and by 90° in all dimensions for 3D experiments. After zero filling and Fourier transformation, the final matrix had 1024, 256, and 256 points along the F_3, F_2, and F_1 dimensions, respectively, and the 2D HSQC experiments had 4096 and 1024 points along the F_2 and F_1 dimensions, respectively. For temperature coefficient analysis, chemical shifts were first calculated and fitted to a straight line after which the deviations from linearity were used to derive the residual curvatures. The digital resolution in the spectra was ~1.7 Hz /point along F_2. The chemical shift assignment was done using the peak picking macro of Felix, which finds the peak maximum using an interpolation procedure. As a measure of curvature, the experimental data (or, equivalently, the residuals from the linear fitting) were fitted to a parabola, by using Marquardt nonlinear least-squares fitting. The protons for which the second-order coefficient (c in the equation $y = a + bx + cx^2$) differed from zero as described by Tunnicliffe et al. were treated as having curved temperature dependence (*33*). The R_2 values were extracted by fitting the peak intensities to the equation, $I(t) = B \exp(-R_2 t)$. Steady state ^1H-^{15}N NOE was calculated as a ratio of intensities of the peaks with and without proton saturation. The errors in the NOEs were obtained using the root-mean-square value of the background noise as described by Farrow et al. (*32*).

RESULTS

Resonance Assignments. The overlay of the HSQC$ spectra of DLC8-WT (wild type dimer) and S88A mutant protein at 27 °C, at pH 7.0, are shown in Figure 1A. The similar spectral features for WT and mutant protein under the given experimental conditions suggest that the protein remains as a dimer even after mutation; this is in contrast to the situation in DLC1 (*20*) where the mutant showed extensive line broadening effects. This was interpreted to indicate dimer−monomer equilibrium in the mutant. Sequence specific resonance assignments of the WT protein have been reported previously (*6*). Majority of the assignments of S88A mutant were derived from simple transfer from those from WT protein. However, on a few occasions where movements of peaks resulted in some ambiguities, the assignments were done by observation of sequential connectivities using CBCANH and CBCA(CO)NH experiments.

S88A Mutant DLC8 Protein of Drosophila Is a Stable Dimer. It is known that certain mutations on the DLC8 dimer result in the dissociation of the dimer (*21, 30*). In order to check the effect of S88A mutation on the DLC8 dimer, we performed gel filtration studies at pH 7 on the mutant protein and compared them with those on the WT dimer and monomer (DLC8 is a monomer at pH 3). The chromatograms are shown in Figure 1B. A single peak for the S88A mutant at the same position as that for the WT dimer indicates that the S88A mutant is a stable dimer. Hence, under our experimental conditions, the S88A mutant remains as a pure dimer. Furthermore, the gel filtration experiments were recorded with different concentrations, namely, 100 and 600 μM protein, and in both cases, the peaks overlay exactly with the same width indicating the absence of another species

in exchange (data not shown). This is in sharp contrast to the results reported by Song et al. (*20*) on the DLC1 protein, the human counterpart of DLC8. The gel filtration chromatogram of S88A mutant of DLC1 showed two peaks, one at a molecular weight higher than that of the dimer and the other in between those of the dimer and the monomer (Figure 5C of ref *20*). The latter was interpreted to indicate dimer−monomer equilibrium, which was supported by extensive line broadening in the HSQC spectrum of the protein. The former peak was supposed to indicate aggregate formation by the mutant protein.

Chemical Shift Perturbations. Even though the spectra of WT-DLC8 and S88A mutant proteins were so similar that the transfer of assignment was possible, there were small differences in the actual chemical shift values. These indicate small local structural perturbations in the native structure of the dimeric protein upon mutation. Using the changes in amide (ΔH) and ^{15}N (ΔN) chemical shifts, we calculated residue-wise summed chemical shift changes ($\Delta\delta$) according to the following formula:

$$\Delta\delta[(H)^2 + (\Delta N/10)^2]^{1/2} \quad (1)$$

The factor 10 for ^{15}N chemical shift arises as a normalization factor since the overall range of nitrogen chemical shifts is roughly 10 times that of proton chemical shifts for the backbone amides in folded proteins. The results of these calculations are shown in Figure 1C. It is evident that the small disruption at Ser 88 causes significant perturbations along the sequence. Overall, there are 3 regions (aa 53−56, aa 65−72, and aa 87−89) that show noticeable changes in the chemical shifts. These span the C-terminal, the β2 and β3 strands, and the loop connecting β3 to β4. The perturbation at the stretch aa 87−89 is a direct consequence of the mutation, which in fact is expected. However, perturbations at β2 and β3 strands and the loop connecting β3 to β4, which are crucial in maintaining the dimer stability and cargo binding, are consequences of relay of perturbation through the protein structure (see below).

Temperature Dependence of Amide Proton Chemical Shifts. The changes in the amide proton chemical shifts measured as a function of temperature are good indicators of hydrogen bonding in globular proteins and also provide information about the local stability of the protein (*34–36*). While linear dependence is used to infer H-bonding, curved dependence of chemical shifts on temperature indicates the presence of alternative states (*37–39*). We measured the temperature dependence of the amide proton chemical shifts in WT and S88A mutant by recording seven HSQC spectra as a function of temperature in the range 20−40 °C. Both the WT and the S88A mutant proteins are stable dimers in the measured temperature range. Hence, the temperature dependence truly reflects the intrinsic stabilities and local perturbations. The temperature coefficients for the residues that showed linear dependences in WT and S88A mutant proteins are shown in Figure 2A and B, respectively.

The average values of the temperature coefficients of WT and S88A mutant are −3.7 ± 0.2 and −3.4 ± 0.1 (the mutated residue is not considered for the calculation of average values), respectively, depicting that the overall stability features (i.e., backbone hydrogen-bonding features) are similar. To visualize the global/local conformational changes explicitly at the residual level due to mutation, we plotted the temperature coefficients of the residues of WT dimer against those of the S88A mutant (Figure 2C). A residue with the same hydrogen-bonding properties/local environment in both proteins will be on the diagonal, and the perturbed ones will deviate from the diagonal. It is evident from Figure 2C that although most residues fall on the diagonal, some residues such as Arg 4, Lys 5, Met 13, Thr53, Trp 54, Asn 61, Thr 70, and Phe 86 show deviation (>1 ppb/°C) from the diagonal. These indicate that small local stability perturbations do occur along the length of the chain. These residues are marked in Figure 2C. Almost all of these residues are seen to be present in the interconnecting loops between secondary structural elements, and the small perturbations at these sites suggest slight readjustment of the structure.

In the above context, Ser 88 presents an unusual behavior. We compared the temperature coefficients of Ser 88 in the WT dimer with those of Ala 88 in the S88A mutant and of Ser 88 in the DLC8 monomer (at pH 3). The plots of temperature dependence for these residues are shown in Figure 2D. The measured temperature coefficients are −19.8 ± 0.3, −9.3 ± 0.2, and −5.6 ± 0.1 ppb/°C for Ser 88 in WT dimer, Ala 88 in S88A mutant, and Ser 88 in DLC8 monomer, respectively. In general, the temperature coefficients range between (−2 to −4) ppb/K for a strongly H-bonded amide protons and between (−5 to −10) ppb/K for an exposed solvent accessible (random coil) amide protons (*40*). The values obtained in the case of the S88A mutant and DLC8 monomer clearly indicate that aa 88 is solvent exposed and not strongly hydrogen bonded. However, a large value of −19.8 ± 0.3 ppb/°C suggests that the environment of the Ser 88 in WT dimer is highly susceptible to perturbation. None of the other residues, neither in WT nor in S88A mutant, showed such a huge temperature coefficient value (Figure 2A and B). Williamson et al. reported such a large value of the temperature coefficient in the herpes simplex virus glycoprotein D-1 antigenic domain (*41*), and the experiments demonstrated by Andersen et al. (*42*) suggested that this amide proton was in fact involved in a transient hydrogen-bonded structure. Thus, the large temperature coefficient could be attributed to a loss of secondary/tertiary structure on heating. If the large temperature coefficient of Ser 88 is a consequence of transient hydrogen-bonding and due to the loss of secondary/tertiary structure, then Ser 88 should exhibit conformational fluctuations (alternative states). The alternative states accessed by a particular residue can be observed by the procedure based on curved temperature dependence of amide proton chemical shifts (*37*). We tested for the presence of alternative states for Ser 88. We also checked the behaviors of the Ala 88 residue of the S88A mutant and Ser 88 in the DLC8 monomer. All of these results are presented in Figure 2E. It is evident that Ser 88 in the WT dimer does show a curved temperature dependence of amide proton chemical shifts. This was also true at other pH values (pH 6 and 8); these experiments at slightly varied experimental conditions (pH 6 and 8) were performed in order to be more certain about the curved dependence (data not shown). Thus, we conclude that the amide proton in Ser 88 in the WT DLC8 dimer is transiently H-bonded; that it is not a stable H-bond was independently inferred from deuterium exchange studies, wherein the amide of S88 was found to exchange very

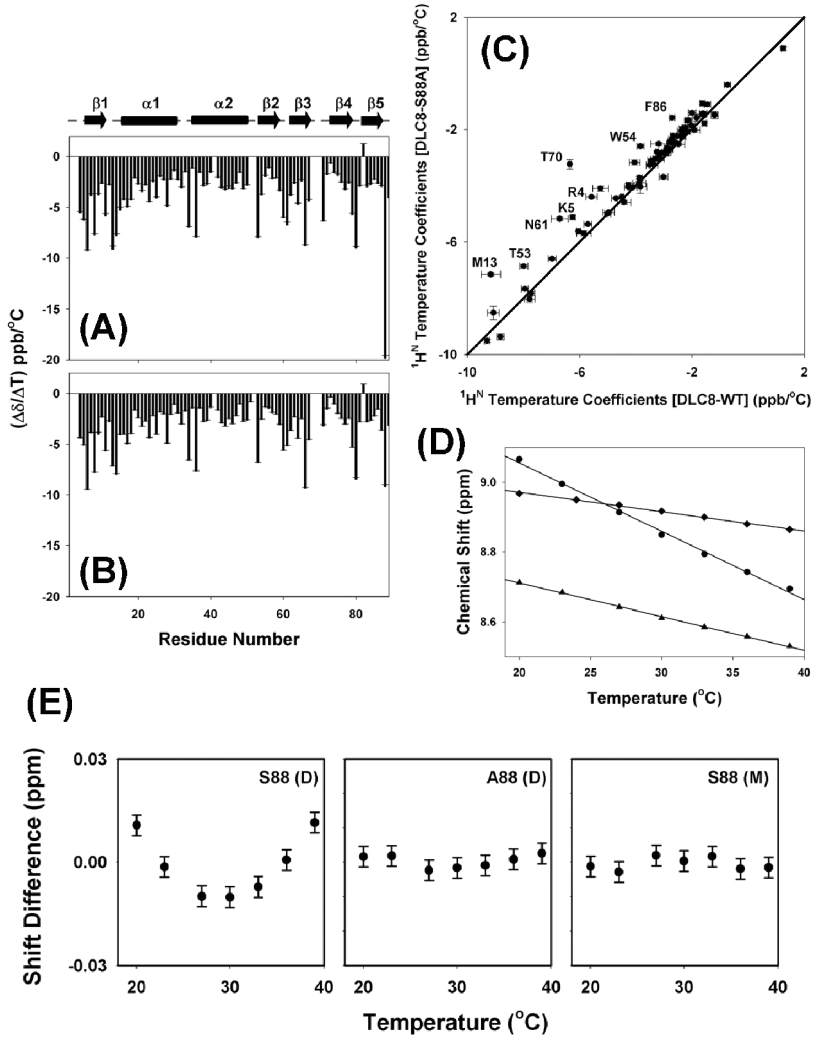

FIGURE 2: Temperature coefficients in DLC8 protein measured at pH 7.0: (A) WT; (B) S88A mutant. The secondary structural elements in the protein are marked above with cylinders (for helices) and arrows (for sheets). (C) Comparison of amide proton ($^1H^N$) temperature coefficients for WT and S88A mutant; the solid diagonal line represents the best linear correlation between the WT and S88A mutant data. Residues Arg 4, Lys 5, Met 13, Thr53, Trp 54, Asn 61, Thr 70, and Phe 86, which show a deviation of >1 ppb/°C from the diagonal suggesting local conformational changes, are marked. The mutation site Ser 88 is not included in the comparison. (D) Graph depicting the temperature dependence of amide proton chemical shifts for Ser 88 in DLC8 WT-dimer (circles), Ala 88 in S88A mutant at pH 7 (triangles), and Ser 88 in DLC8 monomer at pH 3 (diamonds). The solid line represents the best linear fit. (E) Comparison of non linear/linear temperature dependence of amide proton chemical shifts at amino acid position 88 in DLC8 protein: Ser 88 in DLC8 WT-dimer [S88-(D)], Ala 88 in S88A mutant [A88-(D)] at pH 7, and Ser 88 in DLC8 monomer [S88-(M)] at pH 3. The measured chemical shifts were fitted to a linear equation. The residuals (observed value − calculated value according to the linear fit) have been plotted against temperature; the total scale of the *y*-axis is 0.06 ppm; +0.03 to −0.03 centered at zero; and the temperature range is 18−40 °C.

rapidly and the peak was not seen in the HSQC spectrum (Supporting Information, Figure S2). Theoretical simulations carried out in the measured temperature range suggested that the alternative states are within ~2 kcal/mol (Figure S1 of Supporting Information) from the ground state. Furthermore, we believe that this exchange occurs at time scales faster than microseconds since we do not see unusually large transverse ^{15}N relaxation rates for S88 (see below). Since the mutant does not show such a behavior, it follows that Ala 88 in the mutant has a different local environment in the dimer; absence of the H-bond formed by the side chain of Ser 88 to Ser 88′ across the dimer interface and consequent disruption of the structural scaffold can be readily envisaged. The observation that Gly 89 peak in the mutant shifts upfield (Figure 1A) could, in fact, be a consequence of the absence of the H-bond between the nitrogen of Gly 89 and amide of Ala 88, and the consequent structural changes in that region.

Modulation of Conformational Dynamics. Backbone ^{15}N relaxation measurements such as transverse relaxation rate (R_2), and ^1H-^{15}N steady state NOEs, provide direct information on various time scale motions in the protein (*43*). ^{15}N transverse relaxation rates (R_2) serve as useful monitors for local conformational transitions occurring on the milli-to-micro second time scale. Whenever present at particular residue sites, conformational exchange results in conspicuously enhanced R_2 values for those residues. However, the ^1H-^{15}N steady state NOEs are very sensitive to picosecond time scale motions. The sequence-wise variation of these relaxation parameters would be extremely valuable in deriving information on residue-specific motional characteristics. In order to investigate the effect of S88A mutation on the overall dynamics of the DLC8 dimer, we measured the transverse relaxation rates and ^1H-^{15}N steady state NOEs on the S88A mutant and compared them with those of the WT

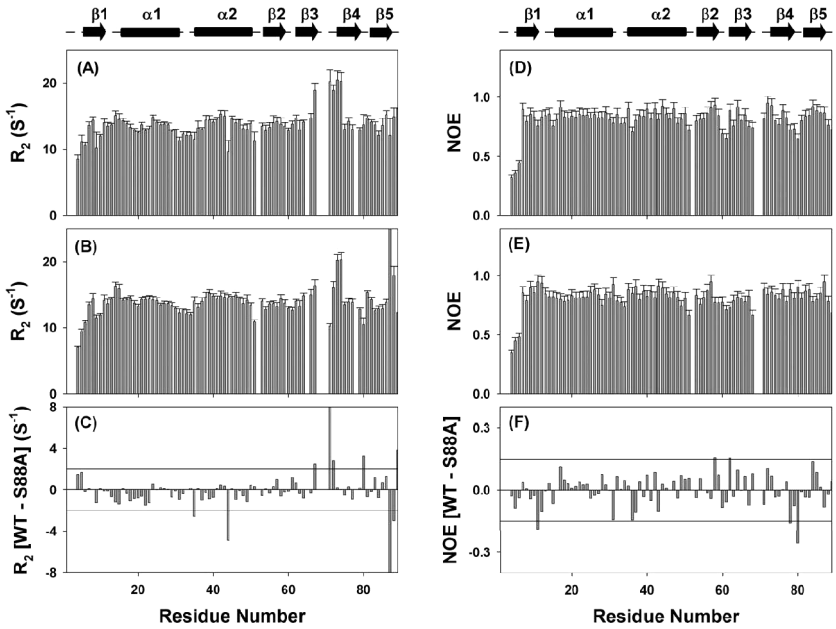

FIGURE 3: Relaxation data of DLC8 dimer at pH 7 and 27 °C: residue-wise ^{15}N transverse relaxation rates (R_2) of (A) WT, (B) S88A mutant, and (C) difference of R_2 values between WT and mutant; ^{1}H-^{15}N steady state NOE values for WT (D), S88A mutant (E), and the difference of NOE's between WT and mutant (F). The secondary structural elements in the protein are marked above with cylinders (for helices) and arrows (for β-strands).

dimer. The residue-wise R_2 values for the wild type dimer, the S88A mutant, and the differences between these are shown in the top (A), middle (B), and bottom (C) panels, respectively, in Figure 3. Similar data for the ^{1}H-^{15}N steady state NOEs are shown in Figure 3D−F. It is evident from Figure 3C and F that there are changes in both the R_2 values and ^{1}H-^{15}N steady state NOEs on mutation. There are both positive and negative changes in R_2 values (Figure 3C), and these indicate changes in flexibility occurring on different time scales in different parts of the protein. Enhancement of milliseconds−microsecond time scale motions would cause negative difference, and enhancement of higher time scale motions would cause a positive difference in Figure 3C. Assuming a conservative cutoff of ~15% of the average value for the change to be considered meaningful (note that this is more than twice the average error in the individual values themselves), we observe that the mutation of Ser to Ala at position 88 induces enhanced conformational exchange in the aa stretch 87−89 and large R_2 values at Lys 87 and Ala 88 in the S88A mutant compared to that in the WT protein (Figure 3C). A similar conclusion is evident at position 44, which is in the middle of the α2 helix. However, there is an enhanced conformational flexibility (positive values in Figure 3C) in the region aa 67−72. Earlier studies revealed that this stretch exhibits conformational exchange in the milliseconds−microsecond time scale (*6, 44*). The conformational dynamics in this region is essential as this loop acts as the channel for the incoming target to bind (*44*). Thus, alteration of dynamics in this region would directly influence the cargo binding adaptability of the DLC8 dimer. The steady state NOEs, which reflect upon picosecond time scale motions, show small but many changes across the length of the chain (Figure 3F). At one particular region, namely, aa 78−80 (loop connecting β4 and β5), there appears to be a noticeable increase in the motions as a consequence of the perturbation.

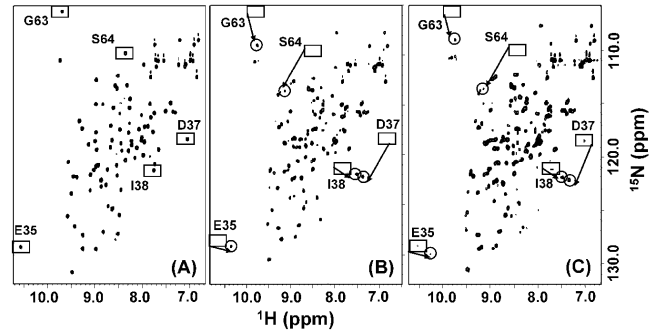

FIGURE 4: ^{1}H-^{15}N HSQC spectra of DLC8. (A) free S88A-DLC8 at pH 7. (B and C) WT in the presence of peptide at pH 7 (B) and S88A-DLC8 in the presence of peptide at pH 7 (C). Peak shifts for a few residues, E35, D37, I38, G63, and S64, are shown for illustration. Squares identify the peaks in the free protein, and circles identify the peaks in the protein−peptide complex. Arrow directions indicate the movement of peaks upon binding to peptide.

Peptide Binding Studies. We compared the cargo binding efficacy of S88A with that of the WT protein at pH 7 by saturating (~1:2.5 ratio of protein:peptide) with a 11-residue fragment of IC74 (dynein intermediate chain), containing the binding motif (K/R)XTQT. HSQC spectra were recorded with and without the peptide. Figure 4A shows the spectrum of free S88A protein at pH 7, and Figure 4B and C shows the spectra of WT and S88A proteins, respectively, in the presence of the peptide. The HSQC spectrum at pH 7 in the presence of the peptide (Figure 4B) has nearly the same number of peaks as the spectrum in the absence of the peptide (Figure 4A), though some peaks have shifted positions because of peptide interaction. These shifts are similar to those reported by Lo et al. (*17*) using peptides containing the same binding motif. In the figure (Figure 4B), we show only a few of those distinct peak shifts (G63, S64, E35, D37, and I38; squares and circles identify the peak positions in the free and peptide bound protein, respectively) for the sake of clarity, but these suffice to demonstrate the binding effects

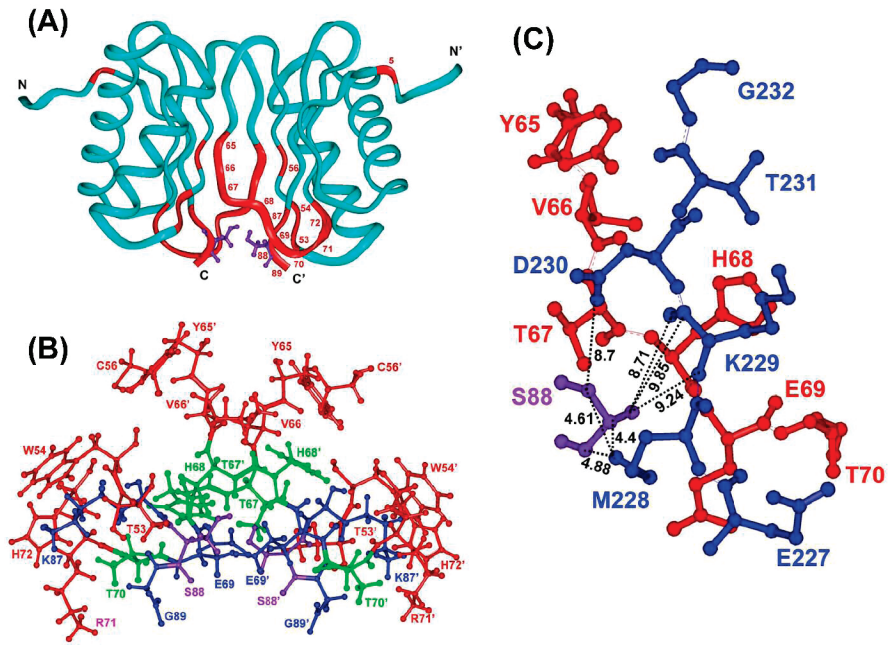

FIGURE 5: (A) Residues exhibiting chemical shift perturbations (Figure 1C) are marked with red on the three-dimensional structure of the protein (pdb ID: 1f3c). The primed and the unprimed labels distinguish the two monomers. Numbers for all of the colored residues (red) are only indicated on one of the monomers for better clarity. The side chain of Ser 88 (violet) is also shown on the structure. (B) Zooming in on a particular region of the dimer interface around Ser 88 in the crystal structure (pdb ID: 1cmi) to show accessibility of the phosphorylation site (side chain -OH of Ser 88) and the interactions of side chains and various other residues with Ser 88. Side chains of the residues that are perturbed (Figures 1C or 5A) are only shown for clarity. The different residues are color coded to indicate the proximity of the side chain atoms of the residue to backbone NH of ser 88. Blue, at least one atom of the side chain is within 2−4 Å; green, at least one atom of the side chain is within the range 4−6 Å; and red, all atoms are beyond 6 Å. (C) Residues involved in the interaction between the DLC8 dimer and the nNOS peptide (Gln 227−Gly 232) (pdb ID: 1cmi). For clarity, only those of DLC8 dimer that show chemical shift perturbation are included. The phosphorylation site (Ser 88, violet) is also shown to illustrate the fact that the phosphorylation site is buried in the binding patch of the DLC8 dimer. A couple of distances from Ser 88 to different residues of the nNOS peptide are marked in order to visualize the proximity of the bound target. The images were produced using Insight II. The DLC8 residues and peptide residues are color coded in red and blue, respectively. For uniformity, Ser 88 is always shown in violet (A−C).

in the spectra. The HSQC spectrum of S88A in the presence of the peptide (Figure 4C) has some more peaks, which indicates the coexistence of multiple species. Many of the peaks can be identified with the free dimer, indicating that the ensemble consists of both bound and free dimer. For example, peaks due to E35, D37, and I38, which had moved to positions indicated by circles on peptide binding, acquire some intensity at their positions in the free dimer (indicated by squares). This clearly indicates that the efficacy of binding has reduced in the S88A mutant compared to that of the WT (Figure 4C). However, the major species is still the bound species as is evident from the low intensities of the peaks belonging to the free protein. These results demonstrate that perturbations at Ser 88 can modulate the binding efficacy of the DLC8 dimer.

DISCUSSION

Relay of Perturbations Due to S88A Mutation across the Length of the Dimer Interface. As discussed above, the S88A mutation causes structural and dynamics perturbations in the DLC8 dimer. The temperature dependence of amide proton chemical shifts suggested that Ser 88 is transiently H-bonded and accesses alternative states. This, in fact, provides a mechanism for the relay of perturbations from the Ser 88 site. To understand these changes, we mapped the chemical shift perturbations (Figure 1C) on the native structure of the protein with red color and annotated for clarity in Figure 5A. Interestingly, the perturbations are seen to be essentially localized at the dimer interface. Even more interestingly, the mutation, which is at the extreme C-terminal, seems to perturb the dimer interface to a significant extent. In order to visualize these features, we analyzed the packing of the Ser 88 residue with those of the neighboring residue side chains (closer in space). The side chain packing of perturbed residues and Ser 88 are shown in Figure 5B. The crystal structure shows that the Ser 88 OG atom is packed against the imidazole ring of His 55 and in addition forms a hydrogen bond with the backbone carbonyl of Ser 88′ (Ser 88 of other monomer) (*8, 21*). From Figure 5B, it is evident that Ser 88 is buried inside and packed over side chains of crucial residues at the dimer interface. A closer look at the Ser 88 environment in Figure 5B depicts that Ser 88 is closely packed against the side chains of Thr 67, His 68, and Glu 69 of both the monomers in the dimer. Furthermore, the distance measurements between the backbone and side chain atoms of Ser 88 and those of Thr 67, His 68, Glu 69, and Thr 70 indicated that several atoms of Glu 69 are very close (~2−4 Å), whereas for residues Thr 67, His 68, and Thr 70, there is at least one atom in the distance range of 4−6 Å. All of these residues are perturbed by the S88A mutation as seen from the chemical shift data. The other perturbed residues are slightly farther (>6 Å). All of these are shown in a color coded manner in Figure 5B. This qualitative analysis provides a mechanistic insight into the relay of perturbation from the mutation site; Glu 69 is most easily perturbed, and the disturbance then runs on both sides at

the dimer interface. Then, from Tyr 65 the relay spreads to Lys 44, which is engaged in a side chain H-bond. Thus, Lys 44 also exhibits a large increase in conformational exchange (Figure 3C).

Relevance to Cargo Binding Efficacy. DLC8 is a multi regulatory protein. The crystal structure of the DLC8-nNOS complex indicates that the DLC8 dimer contains two identical target binding grooves on the opposite faces of the protein−dimer interface (*8*). Hence, it has been suggested that DLC8 functions as a linker protein by binding to two different target molecules. In the crystal structure of the complex, residues in the amino acid stretch 65−70 of the DLC8 dimer are in closest vicinity to the nNOS peptide residues (Gln 227−Gly 232) (Figure 5C). Interestingly, the same stretch, aa 65−70, also shows substantial perturbations due to the S88A mutation in the present study (Figure 5A). Ser 88, itself, is buried in the binding patch. Analysis of the DLC8-nNOS structure depicts that backbone and side chain atoms of Ser 88 are closer to the methyl group of Met 228 (∼4−5 Å) of the nNOS peptide, which is involved in the hydrophobic interactions with DLC8 (Figure 5C). But there are no direct short-range contacts with the bound target molecule. Nevertheless, as explained in the previous section, Ser 88 is closely packed against the side chains of Thr 67, His 68, and Glu 69, which play crucial roles in target recognition and binding. Thr 67 forms an H-bond with the side chain of Asp 230. The C═O of His 68 pairs with Lys 229 of the target, as a part of the antiparallel β-sheet between DLC8 and the target. Moreover, backbone nitrogen of His 68 forms a H-bond with the side chain of Lys 229, and the nitrogen of the imidazole ring forms a H-bond with the side chain of Thr 231. This side chain interaction of His 68−Thr 231 is highly crucial for specific target recognition by DLC8. Mutation of Thr 231 to the Gly residue significantly reduced the binding affinity of the nNOS peptide to DLC8 (*45*). Furthermore, the residues of the β3-β4 loop (aa. 69−71) form a hydrophobic groove on one side to accommodate the hydrophobic residues Thr 231, Ile 233, and Val 235 of the nNOS peptide (*8*). Hence, one can conclude that the perturbations at Ser 88 relay to the cargo binding surface through side chain interactions of closely packed residues, and this can modulate the binding characteristics of the DLC8 dimer. Our observation of drop in peptide binding efficacy due to the S88A mutation is in accordance with these effects.

CONCLUSIONS

In summary, we observe that the phosphorylation site, Ser 88, though located at the C-terminal and at the edge of the dimer interface of the DLC8 protein, is fairly buried, forms transient hydrogen bonds, and accesses alternative conformations. A small disruption at this site by way of a point mutation (S88A) significantly modulates the structural and dynamics features at remote places in the dimer through the relay of perturbations. By extrapolation, one can also envisage such effects due to environmental perturbations such as pH, salt, and so forth (*36*). These are seen to influence the target binding efficacy of the protein. Considering the crystal structure of the DLC8-nNOS complex, we provide a rationale as to how even though Ser 88 does not form any direct contacts with the bound target molecule, perturbation at this site can alter the target binding efficacy of the DLC8 dimer. Such a situation can possibly be visualized for other target peptides as well.

It is also interesting to note that the effects of the same S88A mutation in DLC1, the human counterpart of DLC8, reported recently (*20*) are dramatically different. The latter differs from DLC8 at only five locations (human, C2, S21, E23, H41, and K71; *Drosophila*, S2, A21, D23, Y41, and R71), which amounts to a small local perturbation. Hence, the observed differences highlight the sensitivity of the protein to small perturbations, be it internal, as exemplified here, or by extrapolation, external, such as pH, salt changes, and so forth. All of these results provide a rationale for the remote effects of mutations on the one hand and protein's adaptability to different targets on the other. These would clearly have significant functional implications.

ACKNOWLEDGMENT

We thank Dr. Anindya Ghosh-Roy for the DLC8 clone.

SUPPORTING INFORMATION AVAILABLE

Simulations of the dependence of H^N chemical shift variation with temperature (290−315 K) and the ^1H-^{15}N HSQC spectra of the DLC8 dimer at pH 7.0 (A) before adding D_2O and (B) 8 min after adding D_2O. This material is available free of charge via the Internet at http://pubs.acs.org.

REFERENCES

1. Vallee, R. B., Williams, J. C., Varma, D., and Barnhart, L. E. (2004) Dynein: An ancient motor protein involved in multiple modes of transport. *J. Neurobiol. 58*, 189–200.
2. Hirokawa, N., Noda, Y., and Okada, Y. (1998) Kinesin and dynein superfamily proteins in organelle transport and cell division. *Curr. Opin. Cell Biol. 10*, 60–73.
3. Holzbaur, E. L., and Vallee, R. B. (1994) DYNEINS: molecular structure and cellular function. *Annu. Rev. Cell Biol. 10*, 339–372.
4. Pfister, K. K. (2005) Dynein cargo gets its groove back. *Structure (London) 13*, 172–173.
5. Vallee, R. B., and Sheetz, M. P. (1996) Targeting of motor proteins. *Science 271*, 1539–1544.
6. Mohan, P. M., Barve, M., Chatterjee, A., and Hosur, R. V. (2006) pH driven conformational dynamics and dimer-to-monomer transition in DLC8. *Protein Sci. 15*, 335–342.
7. Barbar, E., Kleinman, B., Imhoff, D., Li, M., Hays, T. S., and Hare, M. (2001) Dimerization and folding of LC8, a highly conserved light chain of cytoplasmic dynein. *Biochemistry 40*, 1596–1605.
8. Liang, J., Jaffrey, S. R., Guo, W., Snyder, S. H., and Clardy, J. (1999) Structure of the PIN/LC8 dimer with a bound peptide. *Nat. Struct. Biol. 6*, 735–740.
9. Wang, W., Lo, K. W., Kan, H. M., Fan, J. S., and Zhang, M. (2003) Structure of the monomeric 8-kDa dynein light chain and mechanism of the domain-swapped dimer assembly. *J. Biol. Chem. 278*, 41491–41499.
10. Jaffrey, S. R., and Snyder, S. H. (1996) PIN: an associated protein inhibitor of neuronal nitric oxide synthase. *Science 274*, 774–777.
11. Puthalakath, H., Huang, D. C., O'Reilly, L. A., King, S. M., and Strasser, A. (1999) The proapoptotic activity of the Bcl-2 family member Bim is regulated by interaction with the dynein motor complex. *Mol. Cell 3*, 287–296.
12. Puthalakath, H., Villunger, A., O'Reilly, L. A., Beaumont, J. G., Coultas, L., Cheney, R. E., Huang, D. C., and Strasser, A. (2001) Bmf: a proapoptotic BH3-only protein regulated by interaction with the myosin V Actin motor complex, activated by anoikis. *Science 293*, 1829–1832.
13. Fuhrmann, J. C., Kins, S., Rostaing, P., El, F. O., Kirsch, J., Sheng, M., Triller, A., Betz, H., and Kneussel, M. (2002) Gephyrin interacts with Dynein light chains 1 and 2, components of motor protein complexes. *J. Neurosci. 22*, 5393–5402.
14. Naisbitt, S., Valtschanoff, J., Allison, D. W., Sala, C., Kim, E., Craig, A. M., Weinberg, R. J., and Sheng, M. (2000) Interaction

of the postsynaptic density-95/guanylate kinase domain-associated protein complex with a light chain of myosin-V and dynein. *J. Neurosci. 20*, 4524–4534.
15. Lo, K. W., Kan, H. M., Chan, L. N., Xu, W. G., Wang, K. P., Wu, Z., Sheng, M., and Zhang, M. (2005) The 8-kDa dynein light chain binds to p53-binding protein 1 and mediates DNA damage-induced p53 nuclear accumulation. *J. Biol. Chem. 280*, 8172–8179.
16. Schnorrer, F., Bohmann, K., and Nusslein-Volhard, C. (2000) The molecular motor dynein is involved in targeting swallow and bicoid RNA to the anterior pole of Drosophila oocytes. *Nat. Cell Biol. 2*, 185–190.
17. Lo, K. W., Naisbitt, S., Fan, J. S., Sheng, M., and Zhang, M. (2001) The 8-kDa dynein light chain binds to its targets via a conserved (K/R)XTQT motif. *J. Biol. Chem. 276*, 14059–14066.
18. Vadlamudi, R. K., Bagheri-Yarmand, R., Yang, Z., Balasenthil, S., Nguyen, D., Sahin, A. A., den, H. P., and Kumar, R. (2004) Dynein light chain 1, a p21-activated kinase 1-interacting substrate, promotes cancerous phenotypes. *Cancer Cell 5*, 575–585.
19. Yang, Z., Vadlamudi, R. K., and Kumar, R. (2005) Dynein light chain 1 phosphorylation controls macropinocytosis. *J. Biol. Chem. 280*, 654–659.
20. Song, C., Wen, W., Rayala, S. K., Chen, M., Ma, J., Zhang, M., and Kumar, R. (2008) Serine 88 phosphorylation of the 8-kDa dynein light chain 1 is a molecular switch for its dimerization status and functions. *J. Biol. Chem. 283*, 4004–4013.
21. Song, Y., Benison, G., Nyarko, A., Hays, T. S., and Barbar, E. (2007) Potential role for phosphorylation in differential regulation of the assembly of dynein light chains. *J. Biol. Chem. 282*, 17272–17279.
22. Frankel, B. A., Tong, Y., Bentley, M. L., Fitzgerald, M. C., and McCafferty, D. G. (2007) Mutational analysis of active site residues in the Staphylococcus aureus transpeptidase SrtA. *Biochemistry 46*, 7269–7278.
23. Grant, M. A., Lazo, N. D., Lomakin, A., Condron, M. M., Arai, H., Yamin, G., Rigby, A. C., and Teplow, D. B. (2007) Familial Alzheimer's disease mutations alter the stability of the amyloid beta-protein monomer folding nucleus. *Proc. Natl. Acad. Sci. U.S.A 104*, 16522–16527.
24. Piana, S., Laio, A., Marinelli, F., Van, T. M., Bourry, D., Ampe, C., and Martins, J. C. (2008) Predicting the effect of a point mutation on a protein fold: the villin and advillin headpieces and their Pro62Ala mutants. *J. Mol. Biol. 375*, 460–470.
25. Krishna Mohan, P. M. (2007) Unfolding energetics and conformational stability of DLC8 monomer. *Biochimie 89*, 1409–1415.
26. Ishibashi, M., Tatsuda, S., Izutsu, K., Kumeda, K., Arakawa, T., and Tokunaga, M. (2007) A single Gly114Arg mutation stabilizes the hexameric subunit assembly and changes the substrate specificity of halo-archaeal nucleoside diphosphate kinase. *FEBS Lett. 581*, 4073–4079.
27. Stollar, E. J., Mayor, U., Lovell, S. C., Federici, L., Freund, S. M., Fersht, A. R., and Luisi, B. F. (2003) Crystal structures of engrailed homeodomain mutants: implications for stability and dynamics. *J. Biol. Chem. 278*, 43699–43708.
28. Buck, T. M., Wagner, J., Grund, S., and Skach, W. R. (2007) A novel tripartite motif involved in aquaporin topogenesis, monomer folding and tetramerization. *Nat. Struct. Mol. Biol. 14*, 762–769.
29. Riley, P. W., Cheng, H., Samuel, D., Roder, H., and Walsh, P. N. (2007) Dimer dissociation and unfolding mechanism of coagulation factor XI apple 4 domain: spectroscopic and mutational analysis. *J. Mol. Biol. 367*, 558–573.
30. Nyarko, A., Cochrun, L., Norwood, S., Pursifull, N., Voth, A., and Barbar, E. (2005) Ionization of His 55 at the dimer interface of dynein light-chain LC8 is coupled to dimer dissociation. *Biochemistry 44*, 14248–14255.
31. Permi, P. (2004) Coherence transfer in proteins. *Prog. Nucl. Magn. Reson. Spectrosc. 44*, 97–137.
32. Farrow, N. A., Muhandiram, R., Singer, A. U., Pascal, S. M., Kay, C. M., Gish, G., Shoelson, S. E., Pawson, T., Forman-Kay, J. D., and Kay, L. E. (1994) Backbone dynamics of a free and phosphopeptide-complexed Src homology 2 domain studied by 15N NMR relaxation. *Biochemistry 33*, 5984–6003.
33. Tunnicliffe, R. B., Waby, J. L., Williams, R. J., and Williamson, M. P. (2005) An experimental investigation of conformational fluctuations in proteins G and L. *Structure (London) 13*, 1677–1684.
34. Dyson, H. J., and Wright, P. E. (1991) Defining solution conformations of small linear peptides. *Annu. Rev. Biophys. Biophys. Chem. 20*, 519–538.
35. Rose, G. D., Gierasch, L. M., and Smith, J. A. (1985) Turns in peptides and proteins. *Adv. Protein Chem. 37*, 1–109.
36. Krishna Mohan, P. M., and Hosur, R. V. (2007) NMR insights into dynamics regulated target binding of DLC8 dimer. *Biochem. Biophys. Res. Commun. 355*, 950–955.
37. Williamson, M. P. (2003) Many residues in cytochrome c populate alternative states under equilibrium conditions. *Proteins 53*, 731–739.
38. Mohan, P. M., Mukherjee, S., and Chary, K. V. (2008) Differential native state ruggedness of the two Ca2+-binding domains in a Ca2+ sensor protein. *Proteins 70*, 1147–1153.
39. Krishna Mohan, P. M., Barve, M., Chatterjee, A., Ghosh-Roy, A., and Hosur, R. V. (2008) NMR comparison of the native energy landscapes of DLC8 dimer and monomer. *Biophys. Chem 134*, 10–19.
40. Baxter, N. J., and Williamson, M. P. (1997) Temperature dependence of 1H chemical shifts in proteins. *J. Biomol. NMR 9*, 359–369.
41. Williamson, M. P., Hall, M. J., and Handa, B. K. (1986) 1H-NMR assignment and secondary structure of a herpes simplex virus glycoprotein D-1 antigenic domain. *Eur. J. Biochem. 158*, 527–536.
42. Andersen, N. H., Chen, C. P., Marschner, T. M., Krystek, S. R., Jr., and Bassolino, D. A. (1992) Conformational isomerism of endothelin in acidic aqueous media: a quantitative NOESY analysis. *Biochemistry 31*, 1280–1295.
43. Palmer, A. G. (2001) Nmr probes of molecular dynamics: overview and comparison with other techniques. *Annu. Rev. Biophys. Biomol. Struct. 30*, 129–155.
44. Fan, J. S., Zhang, Q., Tochio, H., and Zhang, M. (2002) Backbone dynamics of the 8 kDa dynein light chain dimer reveals molecular basis of the protein's functional diversity. *J. Biomol. NMR 23*, 103–114.
45. Fan, J., Zhang, Q., Tochio, H., Li, M., and Zhang, M. (2001) Structural basis of diverse sequence-dependent target recognition by the 8 kDa dynein light chain. *J. Mol. Biol. 306*, 97–108.

BI800531G